Phys. Status Solidi A **213,** No. 5, 1193–1198 (2016) / **DOI** 10.1002/pssa.201532789

physica status solidi a
www.pss-a.com
applications and materials science

Optical crosstalk analysis of micro-pixelated GaN-based light-emitting diodes on sapphire and Si substrates

K. H. Li[1], Y. F. Cheung[1], C. W. Tang[2], C. Zhao[2], K. M. Lau[2], and H. W. Choi[*,1]

[1] Department of Electrical and Electronic Engineering, The University of Hong Kong, Hong Kong
[2] Department of Electronic and Computer Engineering, Hong Kong University of Science and Technology, Hong Kong, Hong Kong

Received 30 September 2015, revised 25 January 2016, accepted 25 January 2016
Published online 15 February 2016

Keywords confocal microscopy, GaN, light-emitting diodes, optical crosstalk, sapphire, silicon

[*] Corresponding author: e-mail hwchoi@hku.hk, Phone: +852 28592693, Fax: +852 25598738

With the aid of depth-resolved confocal microscopy, the optical crosstalk phenomenon in GaN-based micro-pixel light-emitting diodes (μ-LEDs) on Si substrates are thoroughly investigated and compared with its counterpart on sapphire substrate. Noticeable optical crosstalk is invariably present in GaN-on-sapphire devices as the thick transparent sapphires beneath the μ-LEDs serve as optical waveguides to favor lateral propagation of the emitted light, eventually causing unwanted noise signals. μ-LEDs adopting the GaN-on-Si platform can effectively suppress unwanted optical crosstalk and sustain superior performance at different injection currents, which are well-suited for a wide range of μ-LED applications.

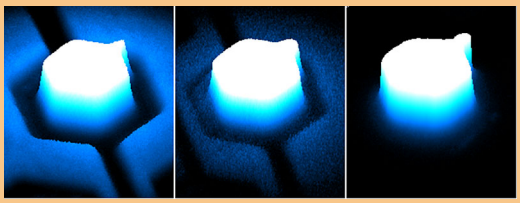

Light intensity maps illustrating crosstalk performances of GaN-on-sapphire μ-LEDs with backsides coated with (left) Al mirror and (middle) black paint, and (right) GaN-on-Si μ-LED, captured by confocal microscopy.

1 Introduction Although sapphire has long remained the predominant substrate material for epitaxial growth of InGaN/GaN light-emitting diode (LED) structures, extensive research efforts devoted to exploring other suitable substrates are conducted in parallel. Silicon is an attractive alternative because of its unique features, including large-size availability at low cost, high thermal conductivity, and possibility of monolithic integration with silicon microelectronics. The major challenges in growing GaN on Si are known to be the appearance of large dislocation densities and wafer cracking due to large lattice and thermal mismatches, but have been effectively alleviated by various strain engineering methods [1–3], such as insertion of intermediate buffer layers and *in situ* depositions of SiN mask, making it possible to realize highly uniform and crack-free structures.

Not surprisingly, GaN-on-Si-based devices are able to compete with the GaN-on-sapphire counterparts in the field of optoelectronics [4–6], including detectors, sensors, and advanced light-emitting sources. The development of micro-LEDs comprised a dense addressable array of miniature LEDs further enable micro-display applications ranging from general lighting to neuroscience, structured light microscopy, maskless lithography and communications [7–9]. In most of the previous reports on micro-pixelated GaN LEDs, the formation of pixels relies on the GaN-on-sapphire platform and typically involves etching through a photolithographically defined masking layer beyond the quantum well region [10, 11]. The pixels can be interconnected to function as a homogeneous emitter, or they can be wired up for individual, matrix or group addressing. While the current μ-LED architecture serves the function of enhancing light extraction well [12, 13], the major flaw of noticeable optical

crosstalk remains unsolved. When a single pixel is addressed, adjacent pixels and regions appear illuminated simultaneously. Such problems could result in functional failure during practical operations, including reduced image fidelity in display applications, flawed data transmission or decreased signal-to-noise ratio in optical communication.

The major cause of optical crosstalk is light channeling along the underlying layers beneath the μ-LEDs that give rise to light coupling to other pixels. To reduce or eliminate crosstalk, these layers must be absent. Devices based on thin-film structures, with the sapphire substrate removed by laser lift-off, have thus been demonstrated, with satisfying results [14, 15]. However, the fabrication of thin-film μ-LED devices is extremely tedious. The fabrication process can be significantly simplified if the substrate is opaque; this can be achieved by fabricating μ-LEDs using the GaN-on-Si platform. In this study, confocal microscopy is employed to investigate the crosstalk performance of GaN μ-LEDs of three different architectures. The mechanism of crosstalk is studied by obtaining depth-resolved confocal emission images from the devices, which vividly illustrate light propagation within the optical layers.

2 Experimental The μ-LED devices in this study are fabricated according to the process flow depicted in Fig. 1(a–d). The LED structures are grown on 6-in (111) Si substrate by metal-organic chemical vapor deposition (MOCVD) with blue-light-emitting InGaN/GaN quantum wells. A semi-transparent current spreading layer consisting of a bi-layer of Ni/Au (5/5 nm) is deposited by electron-beam (e-beam) evaporation, as shown in Fig. 1(a). The array pattern consisting of hexagonal pixels each with dimension of 60 μm is photo-lithographically defined. The unmasked region is etched down to expose the n-GaN surface by inductively coupled plasma (ICP) etching using BCl_3/Cl_2 gas mixtures at a pressure of 5 mTorr as illustrated in Fig. 1(b). The coil and platen powers are fixed at 400 and 100 W, respectively. Prior to metal deposition, a thin SiO_2 film with thickness of 50 nm acting as an electrically insulating layer is e-beam evaporated. The contact area is then exposed by wet etching using dilute hydrofluoric acid through the oxide layer via another photo-lithographically defined mask, as illustrated in Fig. 1(c). The pixels are interconnected in a group-addressable configuration [16], which has been designed for μ-RGB LEDs. Finally, the p- and n-contacts are e-beam deposited, followed by rapid thermal annealing (RTA). The sidewalls of micro-pixels are designed to be fully covered by metallic interconnects to suppress sidewall emission, as illustrated in Fig. 1(d). For comparison, two identical GaN-on-sapphire μ-LEDs with backside coated with Al mirror and black paint are fabricated alongside, called μ-LED with reflector and μ-LED absorber, respectively. Cross-sectional schematic diagrams of the resultant devices are illustrated in Fig. 1(e–g). Micro-photographs shown in Fig. 1(h–j) are the planar views of a group of illuminated pixels of the respective devices driven at 9 mA. The confocal microscopy images are acquired using a Carl Zeiss LSM700 laser-scanning confocal microscope. During measurement, the laser remains off and the illuminated light spots with small focal volume (limited by diffraction) are directly collected from the operating devices through a 5× objective lens with a numerical aperture (NA) of 0.13. After passing through a pinhole with size of 0.3 airy unit, the light intensity is detected and digitized by a photomultiplier tube (PMT). The devices are mounted on a motorized stage to allow 3D scanning across the entire device. Each 2D planar intensity map represents a single optical slice consisting of 256 × 256 data points while the cross-sectional images are constructed by z-stacking optical slices in steps of 10 μm.

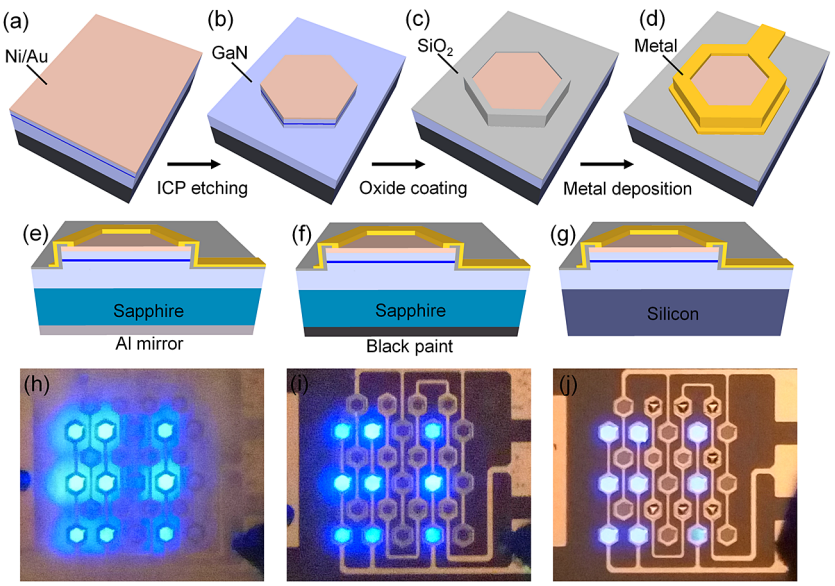

Figure 1 Schematic diagram depicting the fabrication flow of GaN-on-Si μ-LEDs; (a) the starting wafer coated with Ni/Au; (b) exposure of n-GaN region by dry etching; (c) SiO_2 coating followed by wet etching; (d) metal pad deposition by e-beam evaporation. Cross-sectional schematic diagrams depicting architectures of GaN-on-sapphire μ-LEDs with (e) reflector and (f) absorber, and (g) GaN-Si μ-LED. (h–j) Microphotographs showing emission from a group of pixels of the respective devices. All devices are biased at a current of 9 mA.

3 Results and discussion The crosstalk phenomenon associated with typical GaN-on-sapphire μ-LEDs is clearly evident from the microphotograph of the device shown in Fig. 1(h) with a set of pixels illuminated; a strong blue background among the blue-light emitting pixels is clearly observed. To obtain a clear view of intensity distributions from top planes of the emissive μ-LED arrays, confocal microscopic imaging technique is employed and signals from out-of focus planes can be filtered by the pinhole in front of the PMT. As shown in Fig. 2(a), maximum intensity is detected from within a light-emitting pixel (indicated as red) surrounded by a ring of low intensities at the mesa boundary corresponding to the location of the reflective metallic annular contact. The intensity profile along the dashed line shown in Fig. 2(a) is then plotted in Fig. 2(m). It is observed that light emission intensity from the regions beyond the pixel, denoted as noise, can be as high as 19% of the light intensity from the pixel. To investigate how light emitted from the pixels became unwanted background emission, a confocal z-stack scan is performed to probe the intensity variations both within and beyond the optical device. The 2D cross-sectional intensity map shown in Fig. 2(d) is obtained by taking a vertical slice through the middle of a pixel from the 3D intensity graph assembled using the horizontal slices. The position of its active region is indicated with a dotted line in the figure. Above the active region, the intense emission toward the upward direction corresponds to the

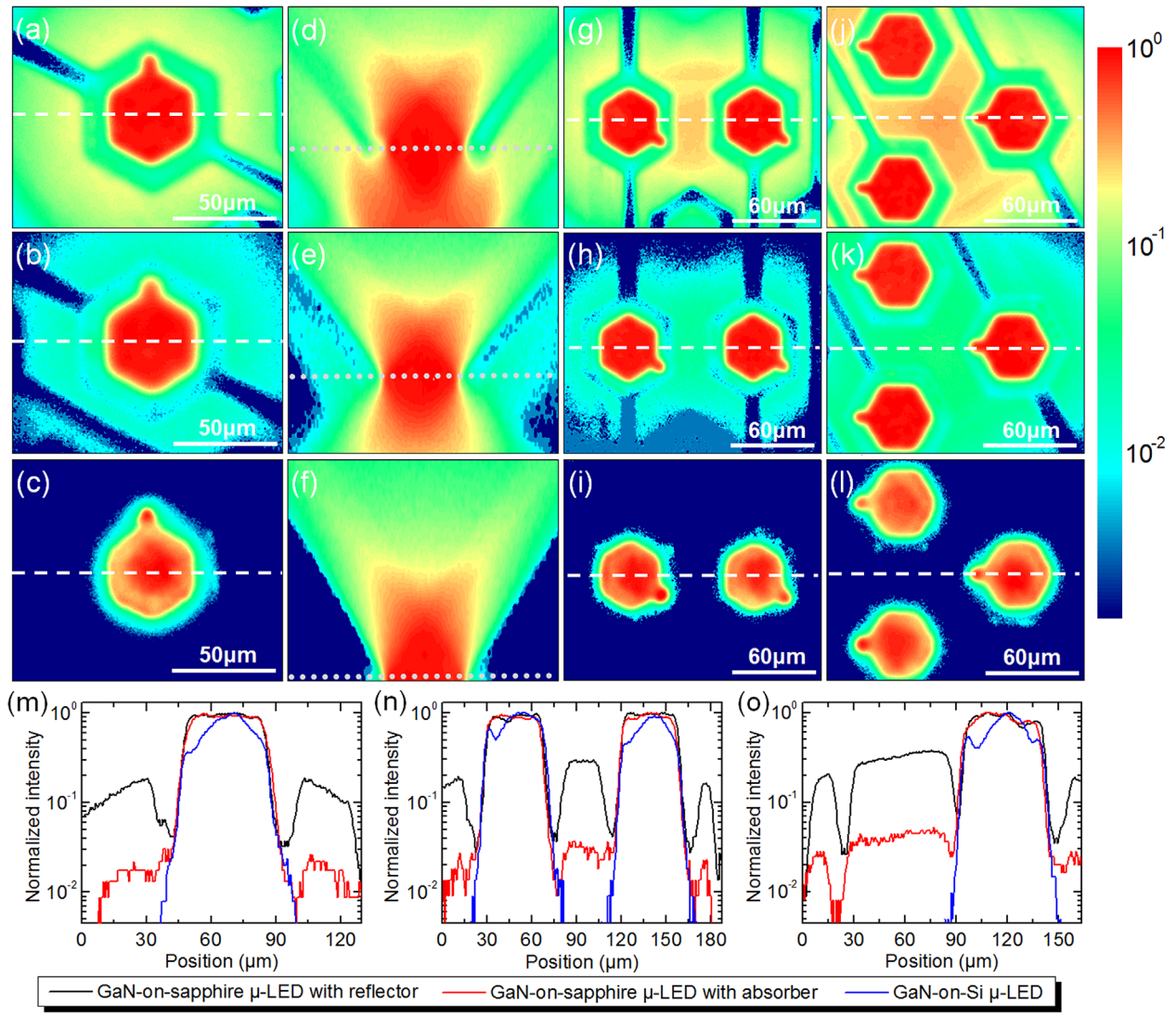

Figure 2 Planar intensity maps of GaN-on-sapphire μ-LEDs with (a) reflector, (b) absorber, and (c) GaN-on-Si μ-LED. (d–f) Cross-sectional emission intensity maps ($130 \times 1000\,\mu m^2$ along x–z plane) of the respective devices plotted on logarithmic scale. Confocal images of emission from (g–i) double and (j–l) triple pixels in respective devices. All intensity maps are normalized and plotted on logarithmic scale. Each pixel is driven at the current of 1 mA. Plots of emission intensity profiles of (m) single, (n) double, and (n) triple pixels along the dashed lines in Fig. 2(a–c), (g–i), and (j–l), respectively.

emitted light extracted from device into free space. Below the active region, the observation of strong intensities of light suggests that large portions of downward light will propagate into the underlying transparent layers. Some of the light rays reflected from the bottom mirror will be able to escape from the top surface if their angles of incidence are smaller than the critical angle. If angles of incidence being larger than the critical angle, total internal reflection occurs. The confined rays will thus channel within the sapphire layer until finding an opportunity to escape, either from the sidewalls or through a rough surface. In other words, the thick transparent sapphire substrate serves as a waveguide to facilitate light propagation along the lateral direction, giving rise to noise in the form of background emission.

The extent of optical crosstalk is further investigated by collecting similar confocal intensity maps across adjacent pixels on a single focal plane. Figure 2(g and j) shows the intensity maps of two and three adjacent illuminated μ-LED pixels separated by ~100 μm. Obviously, the crosstalk effect becomes more pronounced when multiple μ-LED pixels are illuminated simultaneously. Emission intensity profiles along the dashed lines shown in Fig. 2(g and j) are also plotted in Fig. 2(n and o), respectively. The extents of optical crosstalk are then quantified by the signal-to-noise (S/N) ratio evaluated from the ratio of maximum signal intensity (signal within a pixel) to maximum noise intensity (signal beyond a pixel). Compared with the single μ-LED pixel, the peak intensities of noise increase by 58 and 100%, thus resulting in significant reduction of S/N ratios (3.3 and 2.6) for double and triple μ-LEDs pixels, respectively.

Based on the above findings, the major cause of optical crosstalk can be identified to be optical reflections and confinement within the thick transparent sapphire substrate. To minimize such reflections and confinement, metal coatings on the sapphire faces of the devices are replaced by a black paint coating. The microphotograph of such a device shown in Fig. 1(j) indicates that background noise is highly suppressed while the cross-sectional intensity map shown in Fig. 2(e) confirms that the bottom non-reflective coating suppresses reflections of the downward-emitted light from the active region. However, as illustrated in Fig. 2(e and g), noticeable amount of emission from the in-between regions (corresponding to S/N ratios of 27.6 and 19.1, respectively) can still be detected, meaning that crosstalk is not fully eliminated in this design.

As optical channeling occurs in the GaN and sapphire layers, and as the sapphire (of hundreds of microns) is much thicker than the GaN epilayer (of several microns), it is necessary to avoid the emitted light from coupling into the thick transparent substrate. Replacement of the transparent substrate with an absorbing substrate may thus be an effective solution. Incidentally, GaN LED structures grown on Si substrates are becoming increasingly common, with quantum efficiencies comparable to their sapphire counterparts. As such, identical μ-LED devices are fabricated on GaN-on-Si LED wafers following an identical fabrication process. The pronounced improvement in optical crosstalk performance is evident from the microphotograph shown in Fig. 1(j); emission is only detected within the defined micro-pixels while the background appears to be completely noise-free. The cross-section emission profile, obtained from the confocal *z*-stacks, is plotted in Fig. 2(f). Compared with the devices on sapphire substrates, the massive amount of downward emission is no longer observed due to the absorption behavior of Si to blue light. The crosstalk-free performance is further confirmed by the intensity profiles shown in Fig. 2(b and c), whereby the intensities detected beyond the pixels drop sharply, contributing to huge S/N ratio of larger than 100. Table 1 summarizes the S/N ratios of the various devices with different number of illuminated pixels.

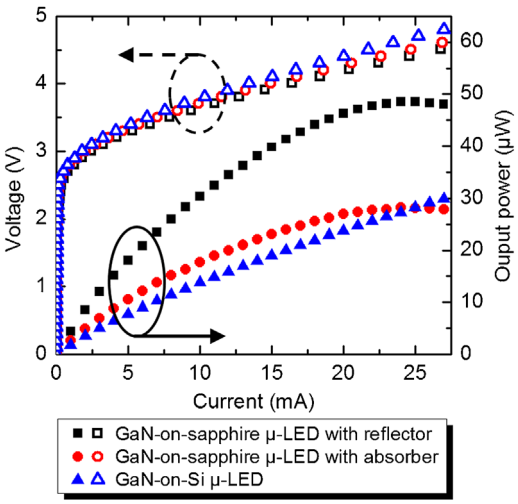

Figure 3 *L–I–V* current–voltage characteristics of devices.

Figure 3 depicts the light–current–voltage (*L–I–V*) characteristics of the devices measured under continuous wave (CW) conditions. The forward voltages at 10 mA are 3.65, 3.72, and 3.76 V for GaN-on-sapphire μ-LEDs with reflector and absorber, and GaN-on-Si μ-LED, respectively. Although their *I–V* characteristics exhibit similar trend in terms of turn-on voltages and dynamic resistances, the light output behaviors are significantly different. The output powers are measured by collecting the emitted light from a single pixel in each of the three micro-pixel LEDs with a 20× objective with numerical aperture (NA) of 0.42 and then detected by a Si-photodiode. At currents below 10 mA,

Table 1 S/N ratios evaluated from different numbers of illuminated pixels of respective devices.

devices	one pixel	two pixels	three pixels
GaN-on-sapphire μ-LED with reflector	5.2	3.3	2.6
GaN-on-sapphire μ-LED with absorber	33.3	27.6	19.1
GaN-on-Si μ-LED	126.1	110	101.5

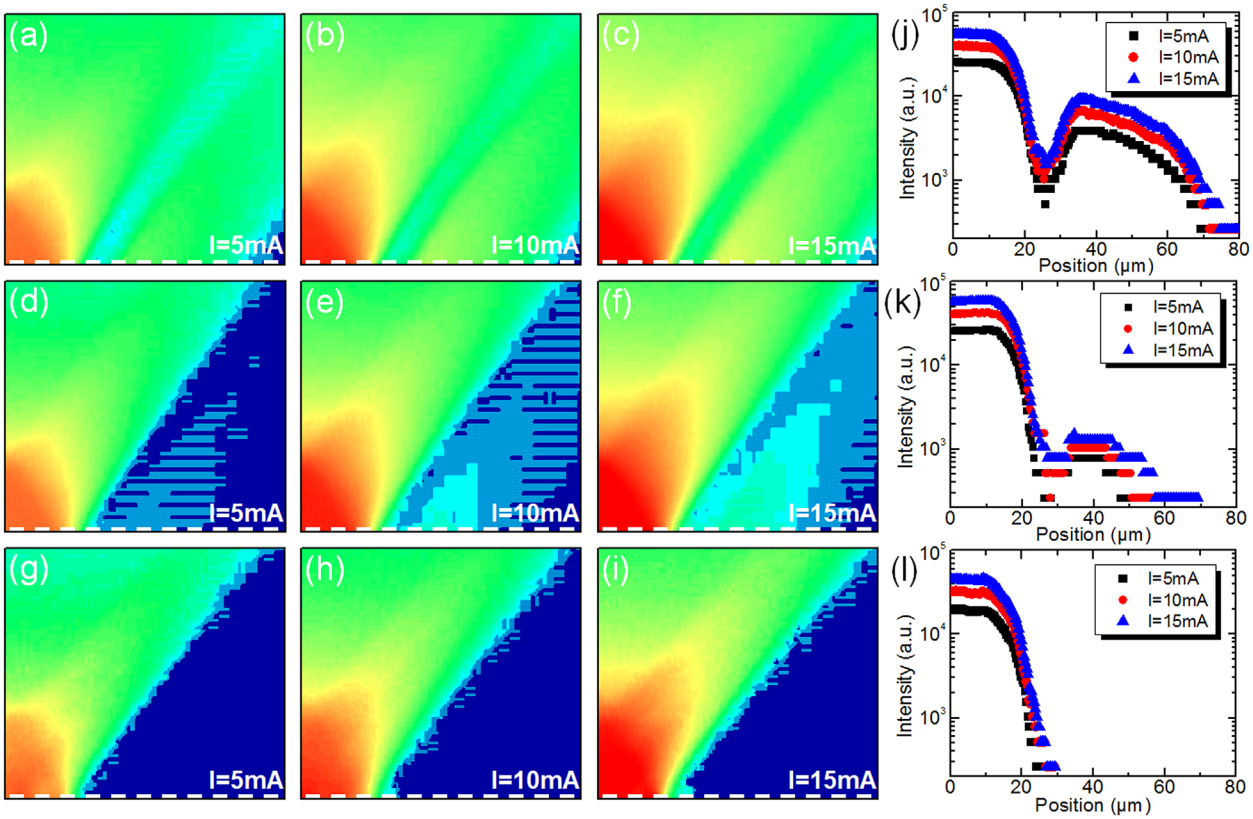

Figure 4 Cross-sectional emission intensity maps ($80 \times 640\ \mu m^2$ along x–z plane) of the GaN-on-sapphire μ-LEDs with (a–c) reflector, (d–f) absorber, and (g–i) GaN-on-Si μ-LEDs driven at varying injection currents. All intensity maps are plotted on logarithmic scale. (j–l) Plots of emission intensity profiles along the dashed lines in Fig. 4(a–c), (d–f), and (g–i), respectively.

the thermal effect is negligible and the light outputs from three devices increase linearly with increasing current. The GaN-on-sapphire μ-LED with reflector emitted ~1.7 and ~2.2 times more light than the devices with absorber and the GaN-on-Si μ-LED, respectively, attributed to the reflection of light by the mirror. With further increase of the injection current, the light output of the GaN-on-sapphire devices shows a trend of saturation due to a device self-heating effect. On the other hand, the GaN-on-Si device can still maintain a linear increase in output power since the heat generated from the active region can be more effectively dissipated through the Si substrate with higher thermal conductivity.

While being capable of reflecting downward-emitted light to enhance light output from individual pixels, the Al mirror coating also induces higher noise level with increasing bias currents. To verify this phenomenon, the confocal z-stack images are taken from devices driven at different current levels. The cross-sectional confocal images shown in Fig. 4(a–c) are recorded from a GaN-on-sapphire μ-LED with reflector driven at currents of 5, 10, and 15 mA, respectively. With increasing currents, both the signal and noise intensity levels are observed to be increased, which are highly proportional to each other. As depicted in Fig. 4(d–f), a similar trend can also be observed from the μ-LED with absorber, except that the overall noise levels are dramatically decreased. The S/N ratios under various injection currents are evaluated to be in the ranges of 5–6 and 32–36 for GaN-on-sapphire devices with reflector and absorber, respectively, indicating that there is a constant portion of emitted light being converted to noise. As illustrated in Fig. 4(g–i), noise is not detected from the regions beyond the pixel, implying the GaN-on-Si retains noise-free performance with increasing current. With superior crosstalk behavior and good thermal conductivities, GaN-on-Si is an ideal platform for the development of μ-LEDs for high-contrast display applications, as well as a wide variety of applications requiring noise-free operation.

4 Conclusions In summary, μ-LED devices have been fabricated on InGaN/GaN epitaxial structures grown on Si substrates. The optical characteristics are conclusively investigated by confocal microscopy and compared with their counterparts on sapphire substrates. A thick transparent sapphire substrate facilitates significant amount of emitted light channeling along the lateral direction, which highly contributes to optical crosstalk and results in poor signal-to-noise ratio. The observation of completely dark background among the emitting pixels from GaN-on-Si devices signifies the effective suppression of optical

crosstalk, attributed to the light absorption of the silicon substrate.

Acknowledgement This work is supported by the Theme-based Research Scheme (T23-612/12-R) of the Research Grant Council of Hong Kong.

References

[1] K. Cheng, M. Leys, S. Degroote, M. Germain, and G. Borghs, Appl. Phys. Lett. **92**(19), 192111 (2008).
[2] E. Arslan, M. K. Ozturk, A. Teke, S. Ozcelik, and E. Ozbay, J. Phys. D: Appl. Phys. **41**(15), 155317 (2008).
[3] A. Able, W. Wegscheider, K. Engl, and J. Zweck, J. Cryst. Growth **276**(3–4), 415 (2005).
[4] A. Osinsky, S. Gangopadhyay, J. W. Yang, R. Gaska, D. Kuksenkov, H. Temkin, I. K. Shmagin, Y. C. Chang, J. F. Muth, and R. M. Kolbas, Appl. Phys. Lett. **72**(5), 551 (1998).
[5] K. S. Stevens, M. Kinniburgh, and R. Beresford, Appl. Phys. Lett. **66**(25), 3518 (1995).
[6] C. Xiong, W. Pernice, K. K. Ryu, C. Schuck, K. Y. Fong, T. Palacios, and H. X. Tang, Opt. Express **19**(11), 10462 (2011).
[7] D. Elfstrom, B. Guilhabert, J. McKendry, S. Poland, Z. Gong, D. Massoubre, E. Richardson, B. R. Rae, G. Valentine, G. Blanco-Gomez, E. Gu, J. M. Cooper, R. K. Henderson, and M. D. Dawson, Opt. Express **17**(26), 23522 (2009).
[8] J. J. D. McKendry, D. Massoubre, S. L. Zhang, B. R. Rae, R. P. Green, E. Gu, R. K. Henderson, A. E. Kelly, and M. D. Dawson, J. Lightwave Technol. **30**(1), 61 (2012).
[9] V. Poher, N. Grossman, G. T. Kennedy, K. Nikolic, H. X. Zhang, Z. Gong, E. M. Drakakis, E. Gu, M. D. Dawson, P. M. W. French, P. Degenaar, and M. A. A. Neil, J. Phys. D: Appl. Phys. **41**(9), 094014 (2008).
[10] S. X. Jin, J. Li, J. Y. Lin, and H. X. Jiang, Appl. Phys. Lett. **77**(20), 3236 (2000).
[11] H. X. Jiang and J. Y. Lin, Opt. Express **21**(9), A475 (2013).
[12] H. W. Choi, M. D. Dawson, P. R. Edwards, and R. W. Martin, Appl. Phys. Lett. **83**(22), 4483 (2003).
[13] H. W. Choi, C. W. Jeon, M. D. Dawson, P. R. Edwards, R. W. Martin, and S. Tripathy, J. Appl. Phys. **93**(10), 5978 (2003).
[14] T. I. Kim, Y. H. Jung, J. Z. Song, D. Kim, Y. H. Li, H. S. Kim, I. S. Song, J. J. Wierer, H. A. Pao, Y. G. Huang, and J. A. Rogers, Small **8**(11), 1643 (2012).
[15] K. H. Li, Y. F. Cheung, W. S. Cheung, and H. W. Choi, Appl. Phys. Lett. **107**(17), 171103 (2015).
[16] W. N. Ng, C. H. Leung, P. T. Lai, and H. W. Choi, Phys. Status Solidi C **5**, 2198 (2008).

